Electrolytic Dissolution and Deposition of Overpotentials of Tantalum in KCl Melts

Ippei NAKAGAWA

Government Industrial Research Institute, Nagoya, Hirate-machi, Kita-ku, Nagoya 462

(Received February 24, 1978)

As part of electrochemical studies on tantalum, the electrolytic dissolution and deposition of solid tantalum in molten salt were studies by measuring its overpotentials in a steady state. The measurements were carried out using the dc current polarization technique in the concentration range of 2.00×10^{-4}—2.79×10^{-1} mole fraction at temperatures between 775 and 875 °C. The kinetic parameters (the exchange current densities, the transfer coefficients, the kinetic averaged valences, and the apparent activation energies) were determined for the anodic and the cathodic reactions in the Tafel region. The over-all reaction was indicated as:

$$(m_1+m_2)Ta^{2+} + (2m_1-2m_2)e \rightleftarrows m_1Ta^0 + m_2Ta^{4+}$$

The Ta^{2+} ion was previously supposed not to form a complex ion; the Ta^{4+}, however, was a complex ion which decomposed at above 850 °C.

Production of refractory metals by fused salt electrolysis has been intensively carried out. Much information on the chemical equilibria in the metal-molten systems has been accumulated in recent years. However, there have been only a few reports on the kinetic data for the refractory metals such as Zr, Hf, Nb, and Ta. Tanaka and Tamamushi[1] compiled the kinetic data in aqueous and in molten salt systems. However, the kinetic data available for the molten salt systems are skimpy by comparison those available for aqueous solutions.

Randles and White applied a relaxation method[2] to the electrode reactions in molten salts. About same time, Laitinen and Osteryoung used the same ac current technique with a platinum electrode in the LiCl–KCl system.[3] Hill *et al.* measured the impedance of tungsten in Ti(II)–Ti(III) couple in the LiCl–KCl eutectic.[4] Laitinen *et al.* measured the exchange current densities of solid metal electrodes (Cd, Zn, Pb, Bi, Ag, Ni, and Pt) and a redox system of V(II)–V(III) in the LiCl–KCl eutectic.[5] T. Kirihara *et al.* have measured the overpotentials of electrolytic dissolution and deposition of Ag,[6] Zr,[7] and Hf[8] in the NaCl–KCl (equiv mole) melts by a galvanostatic method and have evaluated the kinetic parameters (exchange current densities, transfer coefficients, and rate constents).

In the course of the electrochemical studies on Ta,[9-11] the present work was undertaken to determine the kinetic parameters. The electrode processes of dissolution and deposition of solid Ta in the NaCl–KCl (equiv mole) melts will be discussed along with the results of overpotential measurements in a steady state. The values of overpotentials for these processes are also very important in the electrorefining procedure.

Experimental

Chemicals and Procedures. Tantalum plate and wire (99.9%, Fansteel Co.), and tantalum pentachloride (99.9%, Mitsuwa Chemicals Co.) were used. Sodium and potassium chlorides of extra purity were melted under flowing chlorine and argon for further purification and then stored in a desiccator before use.

Electrodes. A working electrode was constructed by connecting a Ta plate with a surface area of 1 cm^2 with a Ta wire to a spectroscopic graphite rod 0.5 cm in diameter. A counter electrode with a surface area of 3 cm^2 and a reference electrode with a area of 1 cm^2 were made in a way similar to the working electrode.

All the electrodes were set in a quartz vessel ($4.5\phi\times45$ cm). An electrical resistance furnace was used to heat the vessel and the temperature was controlled by a current controller with a Pt–Pt·Rh thermocouple within ±2 °C between 775 and 875 °C.

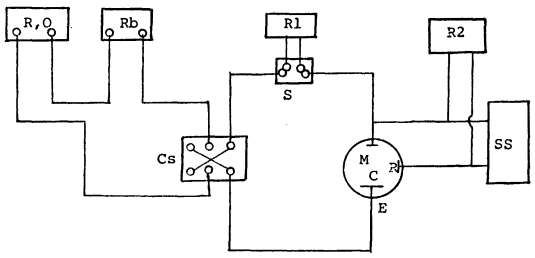

Fig. 1. Schematic diagram of apparatus for measurement of overpotential and resistance of melt.
B: Lead storage battery, O: frequency oscilator, Rb: resistance box, Rl: recorder, R2: recorder, S: shunt, Cs: switch, E: cell, M: measuring electrode, R: reference electrode, C: counter electrode, SS: synchloscope.

Measurement of Ohmic Overpotential. A schematic diagram of the apparatus for measuerment of ohmic resistance of melt is shown in Fig. 1. A precise value of ohmic overpotential caused by ohmic resistance during polarization between the reference electrode and the working one is required to obtain an intrinsic overpotential. That is, $\eta_{total}=\eta_{MR}+\eta_{IR}$, where η_{MR} is the true overpotential and η_{IR} the ohmic one. Both voltage measurements alternating current (20—2000 Hz) and measurements of the initial jump in dc current were employed to determine the value of η_{IR}. The ohmic overpotentials obtained by those methods were in good agreement with each other. A typical example taken by the intial jump method is represented in Photo. 1. The ohmic drop was determined by the gap at the initial part of the curve, as has already been done by other workers.[12] The values of η_{IR} were 0.15—0.27 Ω at various concentrations and temperatures.

Measurement of Overpotential. A schmatic diagram of the apparatus for measurement of overpotemtial is shown in Fig. 1. A galvanostatic method was employed from a low current density to a higher one. The anodic polarization and the cathodic one were measured alternatively in the concentration range of 2.00×10^{-4}—2.79×10^{-1} mole fraction at

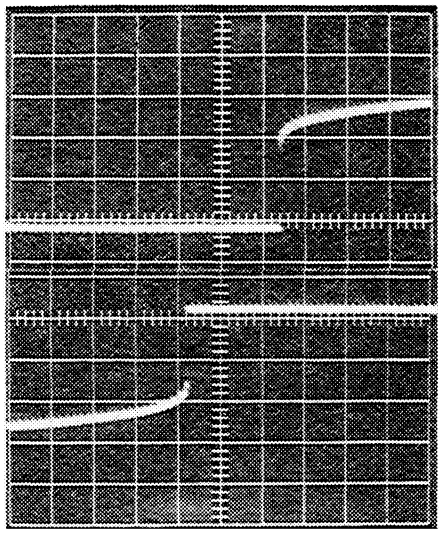

Photo. 1. Potential-time curve for measurement of resistance.
Upper part: dissolution curve, $IR+\eta_{MR}=2.0$ mV
$I=9.4$ mA
$R=0.21\ \Omega$
Lower part: deposition curve, $IR+\eta_{MR}=2.2$ mV
$I=9.4$ mA
$R=0.23\ \Omega$
Vert.: 1 mV/div, Hori.; 0.1 s/div,
Temp: 825 °C. Concn: 2.17×10^{-3} m.f.

temperatures between 775 and 875 °C. All measurements were carried out under an argon atmosphere.

Results and Discussion

Theoretical. The equilibrium reaction between Ta metal and tantalum chlorides has been found experimentally to be

$$Ta^{4+} + Ta = 2Ta^{2+},$$

in the KCl and in the NaCl–KCl (equiv mol) melts.[9-11] Two types of tantalum chlorides, $TaCl_2$ and $TaCl_4$, were found in the equilibrium state. Therefore, the electrode process can not be a simple process like an ordinary electrode reaction which concerns only a simple ion in the solution.

The theoretical treatment for a simultaneous electrode process has been studied by Gray and Cahill.[13] However, this theory is very complicated and it is difficult experimentally to determine the kinetic parameters. Thus we tried to treat the electrode processes for electrolytic dissolution and deposition of solid tantalum with the mobile equilibrium concept which has been explained for zirconium in the chloride system.[14] A more precise consideration will be given elsewhere for the tantalum–chloride system. In this paper, the author describes briefly the concept of mobile equilibrium for the tantalum electrode reactions.

According to emf measurements,[11] Ta^{2+} and Ta^{4+} ions were stable at the electrode surface. For tantalum electrolysis, the charge transfer reactions are usually expressed as

$$Ta^0 \underset{k_{c1}}{\overset{k_{a1}}{\rightleftharpoons}} Ta^{2+} + 2e, \qquad \Delta G_1^\circ < 0 \qquad (1)$$

(ΔG°: free energy)

$$Ta^{2+} \underset{k_{c2}}{\overset{k_{a2}}{\rightleftharpoons}} Ta^{4+} + 2e, \qquad \Delta G_2^\circ < 0 \qquad (2)$$

where k_a and k_c are the rate constants of each direction. The direction right to left means the cathodic reaction (deposition) and the opposite the anodic one (dissolution). The over-all reaction becomes

$$m_1Ta^0 \underset{k_c}{\overset{k_a}{\rightleftharpoons}} (m_1-m_2)Ta^{2+} + m_1Ta^{4+} + 2(m_1-m_2)e, \qquad \Delta G_3^\circ < 0. \qquad (3)$$

When the Process 1 proceeds by m_1 mol, the Process 2 occurs for m_2 mol. If the electrode potentials are high enough,

$$\Delta G_3^\circ = m_1\Delta G_1^\circ + m_2\Delta G_2^\circ < 0,$$
$$-nFE_3^\circ = m_1\Delta G_1^\circ + m_2\Delta G_2^\circ. \qquad (4)$$

The electrode process will proceed according to Eq. 3.

The equilibrium reaction of tantalum is, however $Ta^{4+}+Ta=2\ Ta^{2+}$. So

$$m_1Ta^0 + m_2Ta^{4+} \underset{k_c}{\overset{k_a}{\rightleftharpoons}} (m_1+m_2)Ta^{2+} + 2(m_1-m_2)e, \qquad (3')$$

and $\Delta G_{3'}^\circ = m_1\ \Delta G_1^\circ - m_2\ \Delta G_2^\circ = -nFE_{3'}^\circ$ will occur at lower overpotentials than Eq. 4, because

$$|\Delta G_3^\circ| > |\Delta G_{3'}^\circ|.$$

Accordingly, the charge transfer processes are described as

$$Ta^0 \underset{k_{c1}}{\overset{k_{a1}}{\rightleftharpoons}} Ta^{2+} + 2e, \qquad (1')$$

$$Ta^{4+} + 2e \underset{k_{c2}}{\overset{k_{a2}}{\rightleftharpoons}} Ta^{2+}. \qquad (2')$$

The mobile equilibrium concept for the electrode reaction means a quasi-equilibrium state which involves the electrical work applied to the solution. Therefore, the American convention was adopted to convenience. When mobile equilibrium was established for the Reaction 3′,

$$nFE + \Delta G = 0.$$

Thus, $nFE+\Delta G^\circ+RT\ln a_2^{m_1-m_2}+RT\ln a_4^{m_2}=0$. Accordingly, overpotentials of the cathodic or the anodic process for the Reaction 3′ can be expressed as

$$\eta = E - E_e = \frac{RT}{2(m_1-m_2)F}\{(\ln a_2^{\circ(m_1-m_2)} - RT\ln a_4^{\circ m_2}) - (\ln a_2^{(m_1-m_2)} - \ln a_4^{m_2})\},$$
$$= \frac{RT}{nF}\left\{\ln\left(\frac{a_2^\circ}{a_2}\right)^{(m_1-m_2)} + \ln\left(\frac{a_4}{a_4^\circ}\right)^{m_2}\right\}, \qquad (5)$$
$$= A\eta + (1-A)\eta,$$

where E_e means the equilibrium electrode potential, and a_2° and a_4° are the activities at the equilibrium state for Ta^{2+} and Ta^{4+}, respectively. A is the transfer coefficient and $n=2(m_1-m_2)$ the kinetic averaged valence.

When the diffusion process can be ignored, the relation between the current density and the overpotential can be expressed in wellknown equations for the deposition process:

$$I_c = I_{0c}\{\exp(-A_c n_c F\eta_c/RT) - \exp(A_a^c n_c F\eta_c/RT)\},$$
$$A_c + A_a^c = 1, \quad (6)$$

and for the dissolution process:

$$I_a = I_{0a}\{\exp(A_a n_a F\eta_a/RT) - \exp(-A_c^a n_a F\eta_a/RT)\},$$
$$A_a + A_c^a = 1, \quad (7)$$

Table 1. Exchange currents (I_{0a}, I_{0c})

Concn (mol fract.)	Temp (C°) 755	800	825	850	875
	I_{0a} (mA/cm)²				
2.00×10^{-4}	0.42	0.48	0.50	0.76	1.00
2.17×10^{-3}	1.8	2.4	3.4	4.0	4.6
5.90×10^{-2}	9.0	10.5	12.0	15.0	20.0
1.91×10^{-1}	(31.1	25.0	28.0	21.0	30.0)
2.79×10^{-1}	27.0	30.0	32.0	35.0	42.0
	I_{0c} (mA/cm²)				
2.00×10^{-4}	0.39	0.48	0.50	0.60	0.90
2.17×10^{-3}	1.8	2.4	2.8	3.7	4.0
5.90×10^{-2}	8.0	10.0	12.0	15.0	18.0
1.91×10^{-1}	(13.0	11.0	12.0	13.0	15.0)
2.79×10^{-1}	13.0	16.5	18.0	18.5	26.0

The values in parentheses are uncertain.

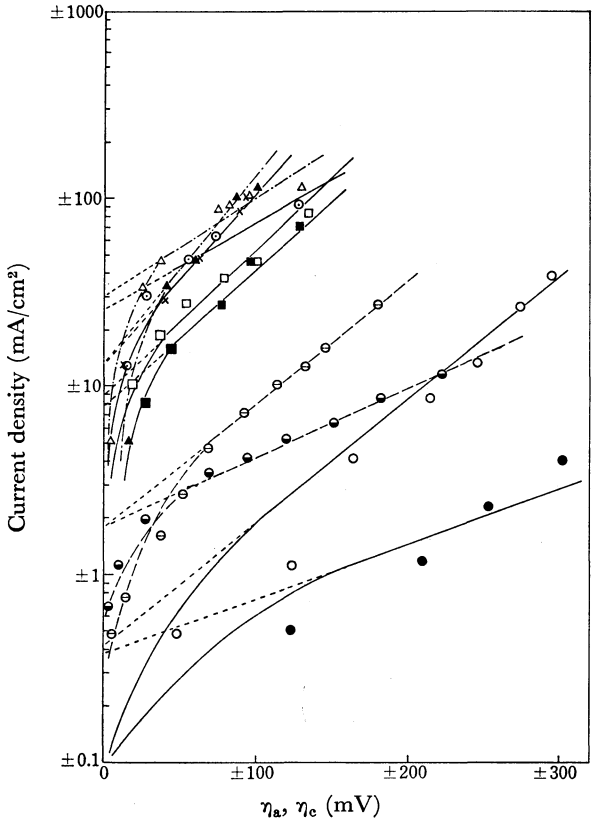

Fig. 2. Relationship between overpotentials and current densities of dissolution and deposition at 775 °C.
Concentration: mole fract.
○ (dissol.), ● (dep.) 2.00×10^{-4}
⊖ (dissol.), ◒ (dep.) 2.17×10^{-3}
□ (dissol.), ■ (dep.) 5.90×10^{-2}
△ (dissol.), ▲ (dep.) 1.91×10^{-1}
⊙ (dissol.), × (dep.) 2.79×10^{-1}

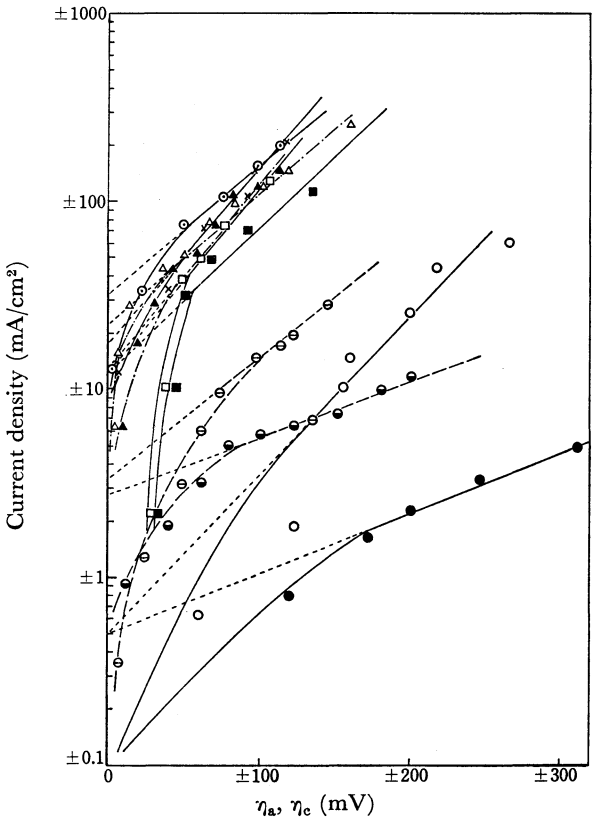

Fig. 3. Relationship between overpotentials and current densities of dissolution and deposition at 825 °C.
Marks are the same as those in Fig. 2.

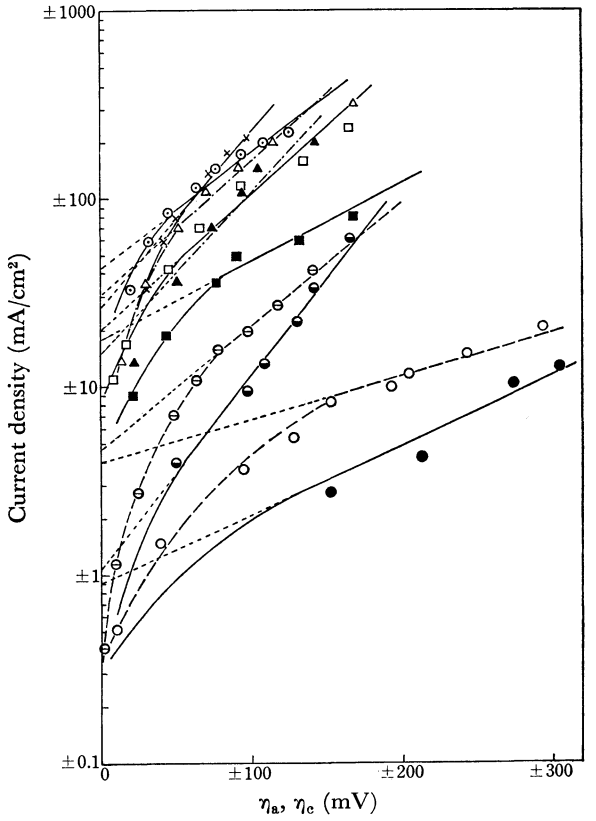

Fig. 4. Relationship between overpotentials and current densities of dissolution and deposition at 875 °C.
Marks are the same as those in Fig. 2.

where subscripts a and c represent the anodic and the cathodic reactions, respectively, I_0 is the exchange current density, I the current density, η the overpotential, A the apparent transfer coefficient, A^a and A^c are the apparent transfer coefficients of the opposing reactions, and F, R, and T have their usual meanings. At high overpotentials, the second terms in Eqs. 6 and 7 can be neglected in comparision with the large values of the first terms. Thus, Eqs. 6 and 7 can be simplified as follows:

$$I_c = I_{0c}\{\exp(-A_c n_c F\eta_c/RT)\}, \quad (6')$$

$$I_a = I_{0a}\{\exp(A_a n_a F\eta_a/RT)\}. \quad (7')$$

The logarithmic expression of Eqs. 6 and 7 gives a wellknown Tafel equation. When the overall faradaic current is equal to zero at $\eta=0$, $I_c=I_{0c}$, $I_a=I_{0a}$. If the electrode reactions are reversible on the Tafel line, $I_{0c}=I_{0a}$.

Exchange Current Densities (I_{0a}, I_{0c}). Plots of log I_a *vs.* η_a are shown in Figs. 2, 3, and 4 for the dissolution process at various temperatures and concentrations; similar relations, log I_c *vs.* η_c, are also represented in Figs. 2, 3, and 4 for the deposition process. The exchange current densities can be obtained from the figures stated above by extrapolation of I_a and I_c in the Tafel region to $\eta_a=0$ and $\eta_c=0$. The values of the exchange current densities thus obtained are tabulated in Table 1. It should be noted that $I_{0a}=I_{0c}$ in the concentration range of 2.00×10^{-4}—2.17×10^{-3} mole frac., and a slight difference between I_{0a} and I_{0c} was observed in the range of 5.90×10^{-2}—2.79×10^{-1} mole fraction. The accuracy of the exchange current densities was estimated to be ±0.2 mA/cm^2 at lower concentrations and ±2 mA/cm^2 at higher concentrations (5.90×10^{-2}—2.79×10^{-1} mole fraction).

The values of $A_a n_a$ and $A_c n_c$ were calculated from the slope of each straight line in Figs. 2, 3, and 4, and are given in Table 2. The n_a and n_c values can be calculated if the transfer coefficients A_a and A_c are determined.

Transfer Coefficients (A_a, A_c) and Kinetic Averaged Valences (n_a, n_c). If we can assume that the activity a^{4+} increases and the activity a^{2+} decreases as the anodic overpotentials for the anodic reaction rise, while for the cathodic reaction, the tendensy is reversed, these activities would vary proportionally to the total concentrations, C_o, which are expressed as mole fractions of the solute in the solution. The relation of log I_{0a} *vs.* log C_o, and that of log I_{0c} *vs.* log C_o gave two groups of straight lines, as shown in Figs. 5 and 6. Two values of the transfer coefficients were obtained, for the lower concentrations and for the higher one, respectively; these values are represented in Table 3. The values of n_a and n_c were calculated from the values in Tables 2 and 3, and given in Table 4.

Activation Energies (E_a, E_c). The apparent activation energies for the dissolution and deposition processes are calculated from the relationships between log I_{0a} and $1/T$ and that of log I_{0c} and $1/T$, according to the following equations:

$$I_{0a} = K\exp(-E_a/RT), \quad (8)$$

$$I_{0c} = K'\exp(-E_c/RT), \quad (9)$$

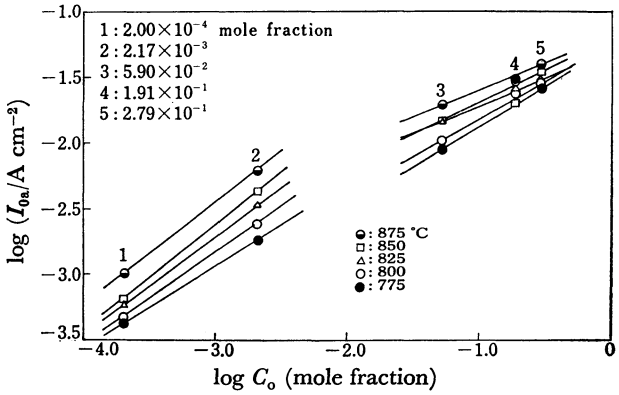

Fig. 5. Relationship between log I_{0a} and log C_o.

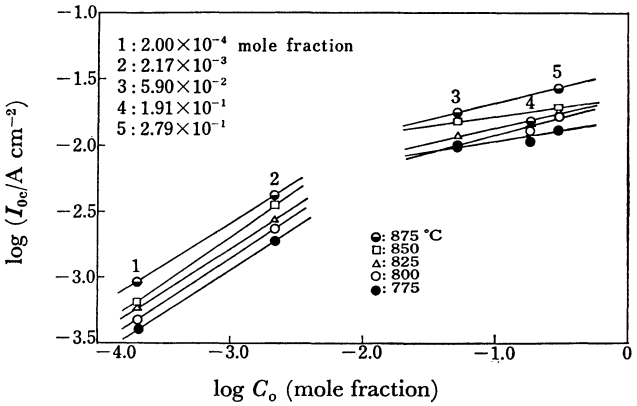

Fig. 6. Relationship between log I_{0c} and log C_o.

TABLE 2. $A_a n_a$ AND $A_c n_c$ VALUES

Concn (mole fract.)	Temp (C°) 775	800	825	850	875
			$A_a n_a$		
2.00×10^{-4}	1.87	1.88	1.84	1.84	2.21
2.17×10^{-3}	1.34	1.37	1.37	1.53	1.50
5.90×10^{-2}	1.62	1.64	(2.18)	1.62	1.75
1.91×10^{-1}	(1.14	1.45	1.65	2.18	1.87)
2.79×10^{-1}	1.41	1.28	1.25	1.10	1.03
			$A_c n_c$		
2.00×10^{-4}	0.63	0.66	0.76	0.85	0.87
2.17×10^{-3}	0.72	0.66	0.68	0.62	0.66
5.90×10^{-2}	1.52	1.37	1.72	1.33	1.18
1.91×10^{-1}	(1.62	2.75	2.25	2.19	1.97)
2.79×10^{-1}	2.32	2.20	1.94	1.81	1.63

The values in parentheses are uncertain.

TABLE 3. TRANSFER COEFFICIENTS (A_a, A_c)

Temp (°C)	A_a a)	A_a b)	$1-A_c$ c)	$1-A_c$ d)
775	0.61	0.70	(0.56)	0.69
800	0.67	0.67	0.27	0.68
825	0.70	0.63	0.38	0.74
850	0.69	0.56	0.24	0.87
875	0.64	0.47	0.38	0.77

The value in parentheses is uncertain. a) Calculated from points 1 and 2 in Fig. 5. b) Calculated from points 3 and 5 in Fig. 5. c) Calculated from points 1 and 2 in Fig. 6. d) Calculated from points 3 and 5 in Fig. 6.

TABLE 4. AVERAGED VALENCES (n_a, n_c)

Concn (mole fract.)	Temp (°C) 775	800	825	850	875
			n_a		
(A) 2.00×10^{-4}	3.0	2.8	2.6	2.7	3.4
2.17×10^{-3}	2.1	2.0	1.9	2.2	2.3
(B) 5.90×10^{-2}	2.3	2.4	3.4	3.0	3.7
2.79×10^{-2}	2.0	1.9	1.9	2.0	2.1
			n_c		
(A') 2.00×10^{-4}	(1.1)	2.4	2.0	3.5	2.2
2.17×10^{-3}	(1.2)	2.4	(1.7)	2.5	1.7
(B') 5.90×10^{-2}	2.2	2.0	2.3	1.5	1.5
2.79×10^{-1}	3.3	3.2	2.6	2.4	2.1

The values in parentheses are uncertain. (A) Calculated by using a) values in Table 3. (B) Calculated by using b) values in Table 3. (A') Calculated by using c) values in Table 3. (B') Calculated by using d) values in Table 3.

where K and K' are the frequency terms, $-E_a$ and $-E_c$ the apparent activation energies for the dissolution and the deposition processes, respectively, and T is the absolute temperature. If the electrode reactions do not change at the experimental temperatures, the relationship between the exchange current densities and the reciprocal temperatures should be linear. In almost all the cases, the values above 850 °C deviate from the straight lines (775—825 °C), as seen in Fig. 7. Thus the temperatures were divided into two regions, 775—825 and 850—875 °C. The activation energies obtained are given in Table 5. The values of E_a and E_c calculated from the straight lines (850—875 °C) were usually larger than those of E_a and E_c (775—825 °C). This fact may suggest that the complex ion[15,16] $[TaCl_6]^{2-}$ is stable at 775—825 °C and decomposes at above 850 °C.

Reaction Mechanism. The electrode reactions on the Tafel line were illustrated by Eq. 5. The stable ions related to the electrode reactions were Ta^{2+} and Ta^{4+} ions. According to Eq. 5, the activity of a_2 decreases and that of a_4 increases with rising overpotentials for the anodic process. For the cathodic process, the opposite trend was observed. The transfer coefficients of $(1-A_c)$ values were chosen to calculate the n_a values, because the n_c values were greater than 5 when the A_c values were used. Therefore, the $(1-A_c)$ will be inserted into the first term and the A_c values into the second term in Eq. 7. The replacement of A_c by $(1-A_c)$ can be ascribed to the relation $(1-A)\eta+A\eta$ in Eq. 5. In other words, the $(1-A_c)\eta_c$ will be assigned to the Ta^{2+} ion and the $A_c\eta_c$ to the Ta^{4+} ion in the cathodic process.

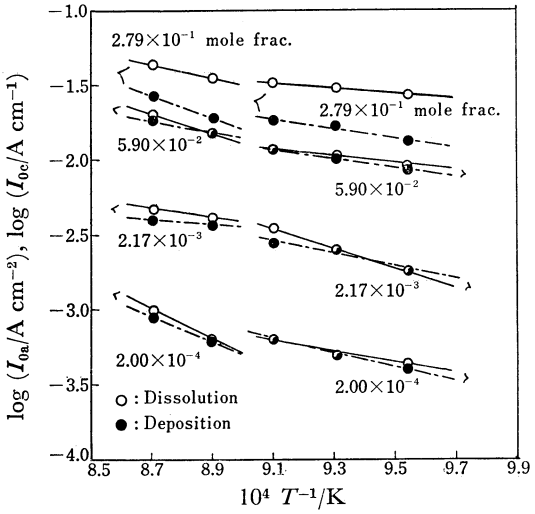

Fig. 7. Relationship between exchange current densities and $1/T^{-1}$/K.

TABLE 5. ACTIVATION ENERGIES (E_a, E_c)

Concn (mole fract.)	E_a a)	E_a b)	E_c a)	E_c b)
	(kcal/mol)			
2.00×10^{-4}	18.8	27.6	21.6	39.1
2.17×10^{-3}	26.7	(11.5)	19.2	(4.6)
5.90×10^{-2}	13.3	23.6	14.6	16.1
2.79×10^{-1}	(7.4)	18.4	14.2	(32.2)

The values in parentheses are uncertain. a) Calculated from the line (775—825°C). b) Calculated from the line (850—875°C).

At lower concentrations, 2.00×10^{-4}—2.17×10^{-3} mole frac., the Tafel relation was established at relatively high overpotentials as seen in Figs. 2, 3, and 4. At higher concentrations, 5.90×10^{-2}—2.79×10^{-1} mole frac., it was established at comparatively low overpotentials. Thus the electrode reactions at lower concentrations will correspond to Eq. 3′ and those at higher concentrations to Eq. 3.

The author wishes to express his thanks to Professor Tomoo Kirihara of Nagoya University for his helpful discussions.

References

1) N. Tanabe and R. Tamamushi, *Electrochim. Acta*, **9**, 963 (1964).
2) J. E. B. Randles and W. White, *Z. Electrochem.*, **56**, 666 (1955).
3) H. A. Laitinen and R. A. Ostertoung, *J. Electrochem. Soc.*, **102** 598 (1955).
4) D. L. Hills, G. J. Hills, L. Young, and J. O. Bockris, *J. Electrochem. Soc.*, **1**, 79 (1959).
5) H. A. Laitinen, R. P. Tisher, and D. K. Roe, *J. Electrochem. Soc.*, **107**, 546 (1960).
6) T. Kirihara, T. Sakakura, M. Iseki, and H. Oshima, Reports of the Faculty of Engineering, Nagoya University, **25**, 47 (1963).
7) T. Sakakura and T. Kirihara, *Electrochem, Soc. Jpn.*, **38**, 423 (1970).
8) T. Sakakura and T. Kirihara, *Electrochem. Soc. Jpn.*, **38**, 496 (1970).
9) I. Nakagawa and T. Kirihara, *Kogyo Kagaku Zashi*, **68**, 1854 (1965).
10) I. Nakagawa and T. Kirihara, *Nippon Kagaku Kaishi*, **1975**, 255.
11) I. Nakagawa, *Nippon Kagaku Kaishi*, **1975**, 958.
12) E. Matisson and J. O. M. Bockris, *Can. J. Chem.*, **37**, 190 (1959).
13) D. Gray and A. Cahill, *J. Electrochem. Soc.*, **116**, 198 (1969).
14) T. Kirihara, I. Nakagawa, and T. Sakakura, 11th Symposium on Chemistry of Molten Salts, 17 (**1977**), (Jpn. Electrochem. Soc.).
15) V. V. Safonov, *Zh. Neorg. Khim.*, **9**, 1406 (1946).
16) T. Suzuki, *Electrochim. Acta*, **15**, 20 (1970).